THEORETICAL AND EXPERIMENTAL INVESTIGATIONS ON LASER HYBRID WIRE ARC ADDITIVE MANUFACTURING

M.Tech Thesis

by

GORLEA THRINADH ANANTH VENKATA TARUN KUMAR

(1902103012)

Department of Mechanical Engineering

Indian Institute of Technology Indore

June 2021

THEORETICAL AND EXPERIMENTAL INVESTIGATIONS ON LASER HYBRID WIRE ARC ADDITIVE MANUFACTURING

A THESIS

Submitted in partial fulfillment of the

requirements for the award of the degree

of

Master of Technology

by

Gorlea Thrinadh Ananth Venkata Tarun Kumar

Department of Mechanical Engineering

Indian Institute of Technology Indore

JUNE 2021

INDIAN INSTITUTE OF TECHNOLOGY INDORE

CANDIDATE'S DECLARATION

I hereby certify that the work which is being presented in the thesis entitled "**Theoretical And Experimental Investigations On Laser Hybrid Wire Arc Based Additive Manufacturing**" in the partial fulfilment of the requirements for the award of the degree of Master of Technology in Mechanical Engineering with specialization in Mechanical Systems And Design submitted in the Discipline of Mechanical Engineering, Indian Institute of Technology Indore, is an authentic record of my own work carried out during the time period from May 2020 to June 2021 under the supervision of Dr. I.A. Palani and Dr. Dan Sathiaraj of Discipline of Mechanical Engineering. The matter presented in this thesis has not been submitted by me for the award of any degree from any other institute.

04/06/2021

G. T. A. V. Tarun Kumar (1902103012)

This is to certify that the above statement made by the candidate is correct to the best of our knowledge.

Dr. I.A. Palani & Dr. Dan Sathiaraj

G. T. A. V. Tarun Kumar has successfully completed his M'Tech Oral Examination held on

Satyanarayan

Signature of Thesis Supervisors

Date: 05-06-2021

Signature of Convener, DPGC

Date:05/06/2021

Girish

K. Eswara Prasad

Signature of PSPC 1 with date:

(Dr. Girish Verma)

Signature of PSPC 2 with date:

(Dr. Eshwar Prasad Korimilli)

ACKNOWLEDGEMENTS

It gives me great pleasure to express our regards and profound gratitude to my project supervisor **Dr. I.A. Palani** & **Dr. Dan Sathiaraj** for their valuable guidance and continuous support throughout project work. My gratitude is also extended towards PSPC members **Dr. Eswara Prasad Korimilli** and **Dr. Girish Verma** for their guidance and cooperation. I would like to thank to Sophisticated Instrumentation Centre of IIT Indore for their support in providing characterization facilities and I would like to thank to all the researchers of Mechatronics and Instrumentation lab for their suggestions and help during experiments. I would gratefully acknowledge the financial aid support received from Ministry of Human Resource and Development. I would like to thank to all the faculty members of the department for providing me all the required information and cooperation which played a vital role in the completion of my project in time. I would also like to thanks my parents, friends and God for their support and strong belief in me. I want to thank my colleagues, especially Ms. Shalini Singh for providing continuous support throughout the journey.

G. T. A. V. TARUN KUMAR

ABSTRACT

Wire arc additive manufacturing (WAAM) is one of the metal additive manufacturing method in which rapid fabrication is possible for components of big size. A significant amount of heat energy is transferred to the work piece during this process, with defined idle period between each deposition layer so that the workpiece cools down during the subsequent layer deposition. This variable cooling rate technique keeps the workpiece from collapsing and maintains a proper inter-pass temperature. The main challenge is to choose an inter-pass ambient cooling time to mitigate the residual stresses induced in the workpiece. The optimum inter-pass cooling time can be outlined by employing experimental and computational iterations. However, before experimental iterations, the material's thermal and mechanical behaviour were investigated using finite element analysis, by introducing DFLUX SUBROUTINE within ABAQUS 6.20 SOFTWARE. The simulation results were analysed and the optimum inter-pass cooling time obtained was 800 sec. These optimized parameters are used for WAAM based 10 Layers stack deposition. The WAAM model developed is also used for preheating thing with mild modifications to observe the change in residual stress. Uniaxial compression test simulation and experiment is done to observe the compressive strength of the experimental samples with various cooling time and pre-heating.

LIST OF PUBLICATIONS

Journal papers (in proceedings)

- Laser Hybrid Wire Arc Additive Manufacturing for fabricating thin sections - Shalini Singh, G.T.A.V Tarun Kumar, Ashish Shukla, I.A. Palani, 2021.

Conference Papers (in proceedings)

- Theoretical Investigations on Influence of Inter-pass cooling conditions on WAAM manufactured parts, ICAMMM, 2021.

TABLE OF CONTENTS

LIST OF FIGURES

LIST OF TABLES

ABBREVIATIONS

Abbreviation	Description
SMA	Shape Memory Alloy
SME	Shape Memory Effect
Ni-Ti	Nickel Titanium
AM	Additive Manufacturing
WAAM	Wire arc additive manufacturing
CAD	Computer Aided Design
GMAW	Gas Metal Arc Welding
SLM	Selective laser melting
PBF	Powder Bed Fusion
MEMS	Micro-Electro-Mechanical Systems
MIG	Metal Inert Gas Welding
WEDM	Wired Electrical Discharge Machining
UTM	Universal Test Machine
NDT	Non-Destructive Techniques
XRD	X-Ray Diffraction

Dedicated to

my father

CHAPTER 1

INTRODUCTION

1.1 Shape Memory Alloys (SMA)

The metals or non-metals possess their own typical material properties like thermal or electrical conductivity, yield strength, machinability etc., and required material is chosen based upon their properties and type of application. But pure metals are chemically reactive and also cannot possess desired material properties with respect to the application terms. So, to enhance the mechanical or chemical properties of the metal, it is combined with the other metals or non-metals and this combination is termed as “alloy”. Alloys are superior and highly desirable when compared to parent metal due to their enhanced material properties like high tensile strength, resistant to wear and tear, high hardness, anti-corrosive and also highly durable in nature. In an alloy mixture, each metal or element lends their own material properties to the compound which exhibits unique properties with much more strength and resistance.

Shape Memory Alloys (SMA) belong to the class of unique materials which has two magnificent novel properties like pseudo-elasticity and shape memory effect (SME). SMA can be deformed into any shape but unlike other materials, SMA’s when heated can return to their original shape. SMA has the ability to regain to original shape from plastic deformation by heat treatment. Twinned martensite, detwinned martensite and austenite are the three crystal structures of SMA. SMA’s can be produced by many ways like Vacuum melting, Powder metallurgy, Electron beam melting, Thin film fabrication, Plasma melting and also by heat treatment methods. Many materials have been found in which we can observe shape memory effect within them like Ni-Ti, Cu-Al-Ni, Cu-Zn-Al, Cu-Sn, Nb-Ti, Cu-Al-Be and Ti-Nb.

1.2 SMA Characteristic's

1.2.1 Shape Memory Effect (SME)

The SMA's existing at low temperature (or room temperature) is in martensite state (twinned martensite), when a load is applied it gets deformed into another shape by getting converted to deformed martensitic state (detwinned martensite). When this deformed SMA is heated, the martensitic state gets converted into austenite and also the initial shape regained. As it gets cooled down, the austenite state returns to initial state i.e., twinned martensite state. This ability to regain its original shape by going through temperature transformation of SMA's is named as "Shape Memory Effect".

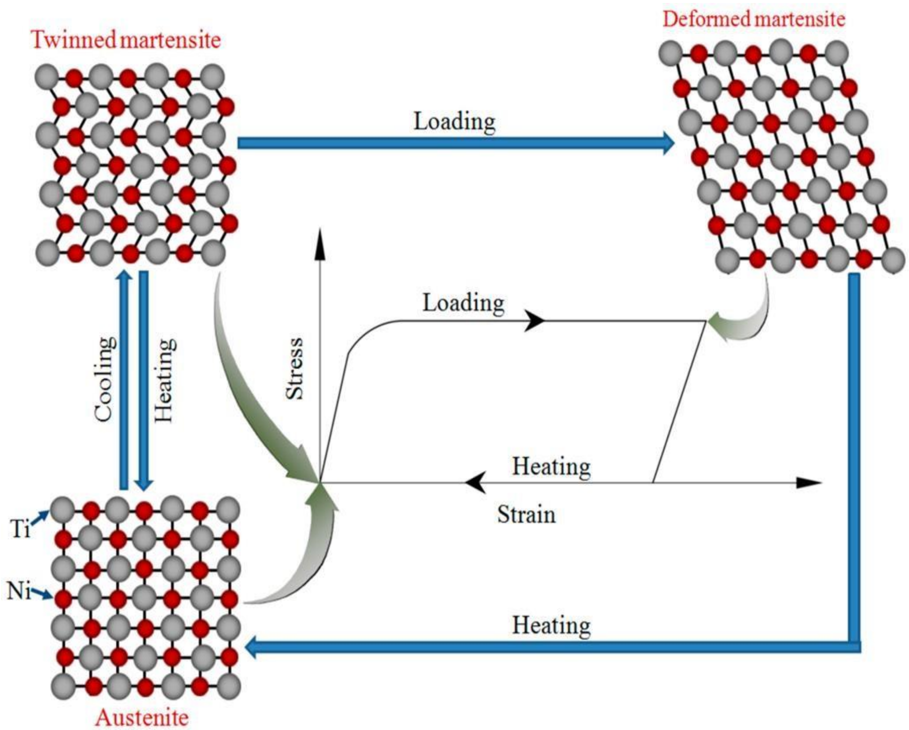

Fig 1.1 SMA Phenomenon of Ni-Ti

1.2.2 Pseudo-elasticity (or Super-elasticity)

The meaning of the word "pseudo-elasticity" is "pseudo" means false and "elasticity" means the ability of material to return to its original shape when it is unloaded. Unlike the shape memory effect, the pseudo-elasticity can be possible without any temperature change, at low temperatures the amount of deformation due to applied stress can be recovered completely after unloading which is not possible in other materials.

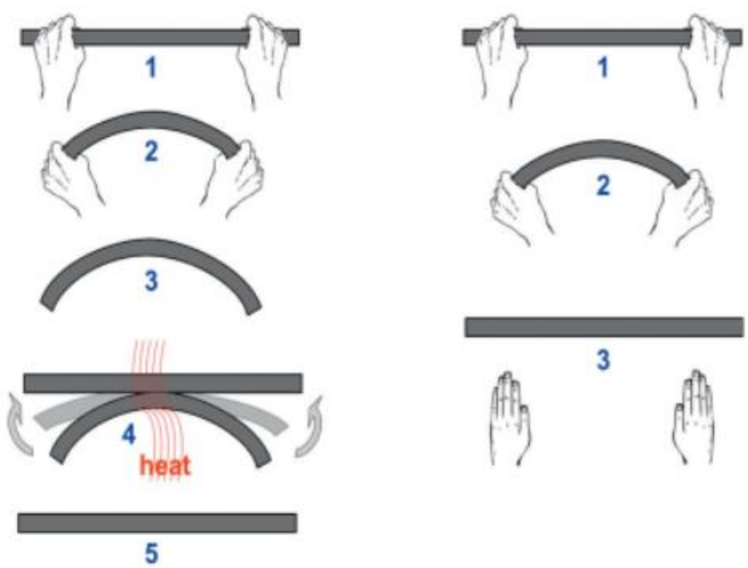

Fig 1.2 Shape Memory Effect and Super-elasticity

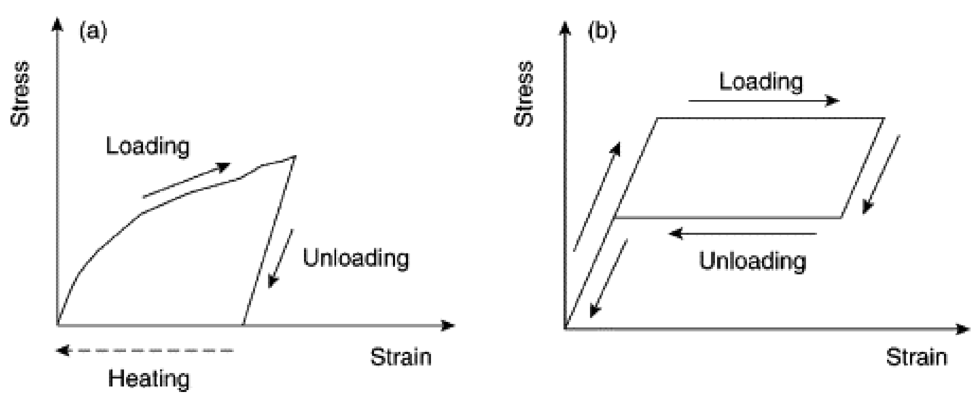

Fig 1.3 Stress-Strain graphs of SME and Super-elasticity

1.2.3 Hysteresis

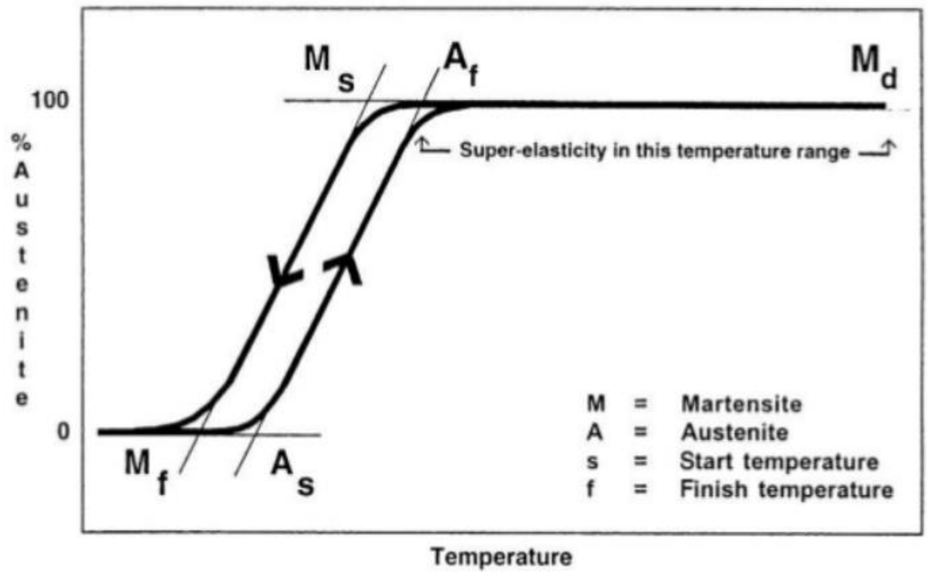

Fig 1.4 Hysteresis curves of SMA

From the graph, it is observed that the path from point M_s to M_f indicates cooling stage and also the path from A_s to A_f indicates heating stage. There exists a difference or delay or lag in transformation temperature from martensite to austenite phase or from austenite to martensite phase by forming a closed loop, named as "hysteresis" loop.

1.3 Applications of SMA

Fire and Safety Applications: Fire-sprinklers, SMA springs in anti-scalding devices.

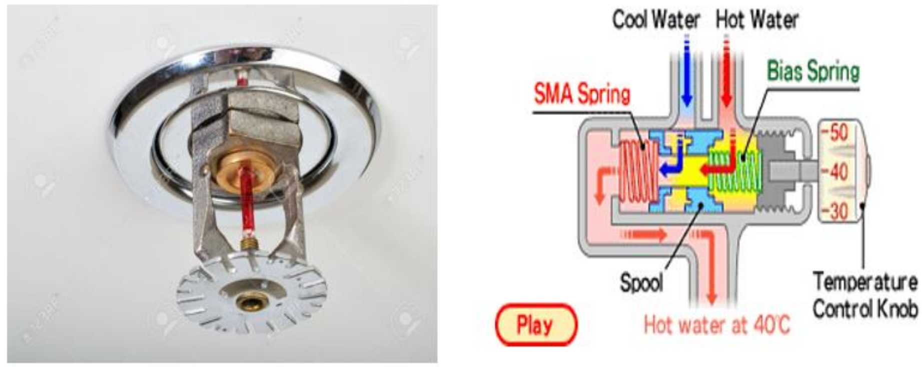

Fig 1.5 Fire sprinklers and SMA springs

Robotics Applications: SMA can be used as actuators for soft robots, micro-engines, micro-pumps, bio-mimic robots etc.,

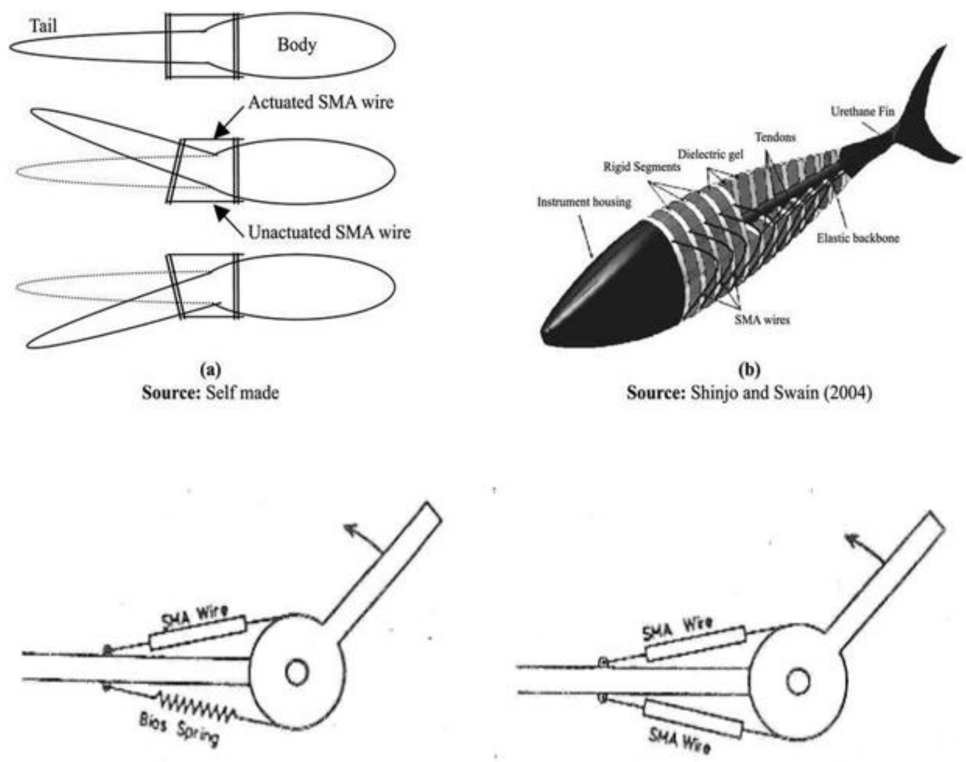

Fig 1.6 SMA actuators in Robotics

1.4 Ni-Ti Applications

Nickel Titanium or Nitinol (Ni-Ti) is a SMA which is composed of Nickel (Ni) and Titanium (Ti) in approximately equal percentages.

Automotive Applications: When compared to other SMAs, the properties of Ni-Ti are more promising and desirable for automotive applications like high strength, resistance to corrosion, electrical resistivity and a high recovery rate of strain. Ni-Ti springs can be used in thermal valves, door lock mechanisms, shock absorbers, Ni-Ti washers for noise reduction and wind-shield wipers.

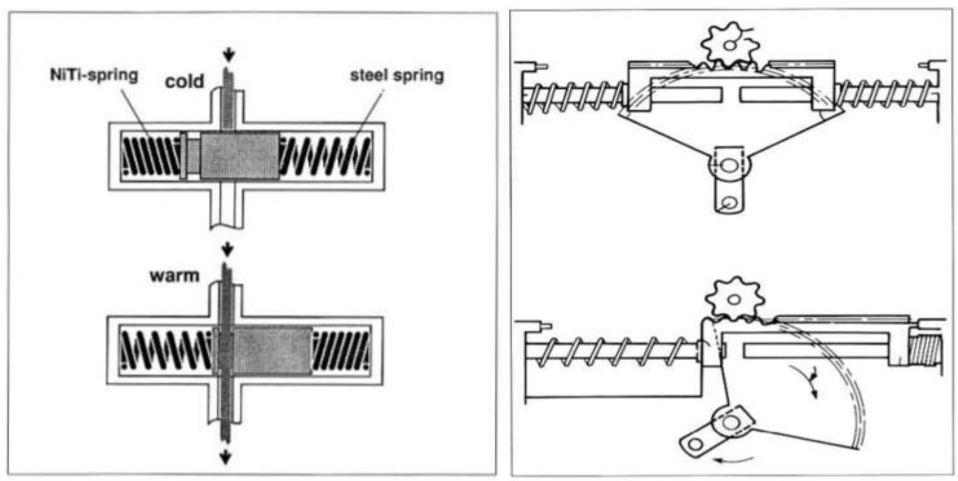

Fig 1.7 Ni-Ti applications in Automotive Lock mechanism

Medical applications: Stents for heart surgeries are made up of Nitinol, tooth clips, eye-glass frames, joining bones.

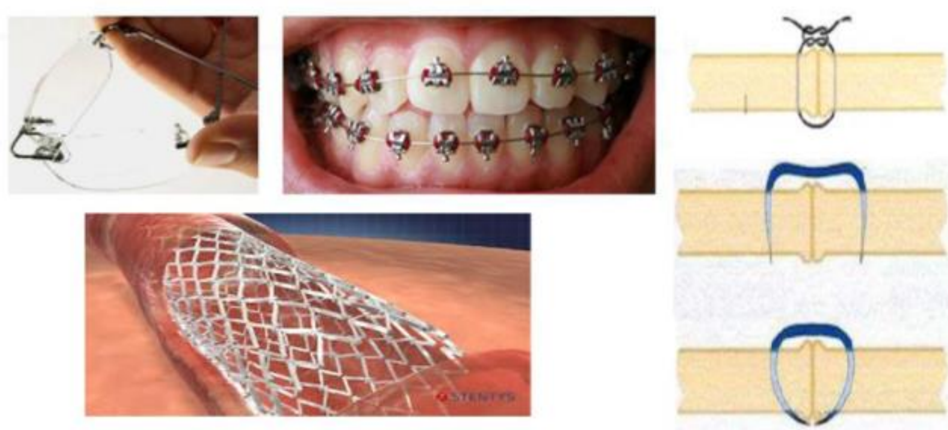

Fig 1.8 Ni-Ti stents, eye-glass frames, teeth clips, bone joints

1.5 Additive Manufacturing (AM)

The term "additive manufacturing" describes "addition of a substance or material upon another by the use of machinery equipment". In additive manufacturing, articles or components are produced in layer-by-layer deposition method. The additive manufacturing is popularly referred as "Three-Dimensional (3 D) printing" which is produced from a Computer Aided Design (CAD) model. This CAD model data is then sent to the Numerical Control (NC) or Computer Numerical Control (CNC) machine to produce the component with respect to the design model.

1.6 Classification of Additive Manufacturing Process

Additive manufacturing process is majorly classified into 3 types:

a) Liquid Based
b) Powder based
c) Solid based

These three categories are again sub-classified into many processes depending upon the form of depositing material and technique involved.

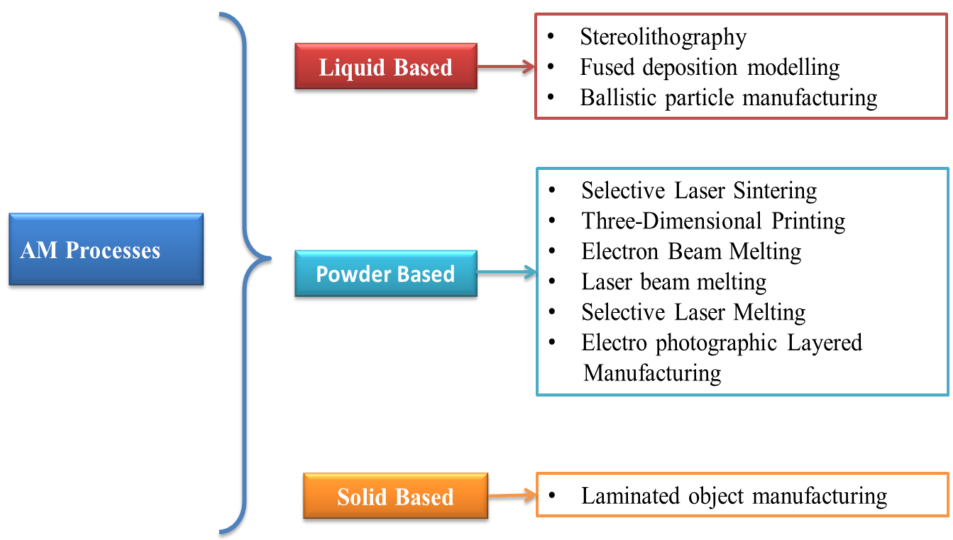

Fig 1.9 Classification of AM process

1.7 Wire Arc Additive Manufacturing

In this process, Gas Metal Arc Welding (GMAW) or Metal Inert Gas (MIG) technique is used in which a metal wire is used as feedstock material to get deposited upon the substrate in the form of layers. Generally, the deposited layers are referred as wall and substrate as base plate. The heat source in this process is the electric arc generated between wire and base plate to melt the feed wire to produce 3D parts. The shielding gas is used to avoid

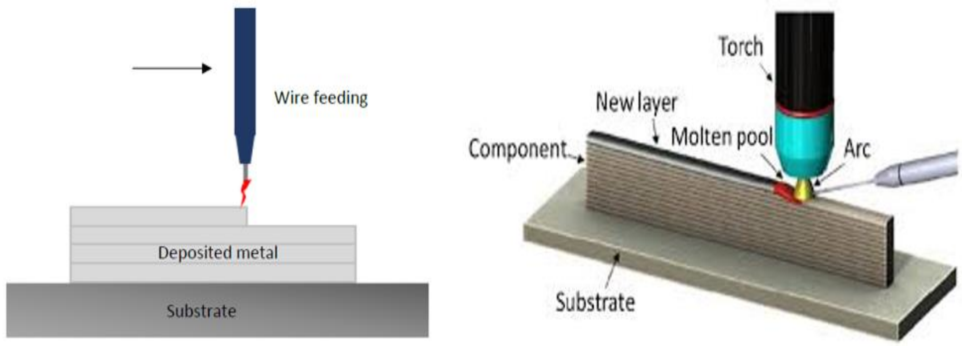

Fig 1.10 WAAM process and its deposition method

oxidation during the deposition, generally inert gases like Argon (Ar) are used as shielding gases with optimum gas flow rate in this deposition process.

When compared to other additive manufacturing process like Selective laser melting (SLM), Powder Bed Fusion (PBF) etc., WAAM has some benefits over them. The WAAM advantages and dis-advantages are as follows:

Advantages

i. Degree of utilization of feed material is very high in this WAAM process with high deposition rate and less material wastage.
ii. Reduced material wastage leads to reduced potential cost and lead time in manufacturing complex parts or components.

iii. Complex parts, near net shape preforms of medium and large sizes can be produced in layer-by-layer deposition method.
iv. The accuracy of the part produced is precise with better surface finish.
v. In producing 3D components through WAAM process, more flexibility is available.
vi. No external machine tooling, dies, casting moulds are not required.
vii. Now a days, laser can used as the heat source to melt and deposit the feed wire over the substrate.

Dis-advantages

i. Compared to other additive manufacturing processes, the heat generated is very high causing residual stresses and distortions in the end component.
ii. Less surface finish can be seen in producing complex parts.
iii. In some cases, skill of the operator and continuous monitoring is essential for successful layers build up or else cracks can be formed.
iv. Post finishing operations are done to remove spatter and excess material on the substrate.

WAAM is an emerging advanced manufacturing technology, with proper optimization parameters and selection of feed material, complex parts with efficient structure can be produced with less material wastage.

CHAPTER 2

MOTIVATION, OBJECTIVES & METHODOLOGY of RESEARCH

2.1 Motivation

Wire arc additive manufacturing (WAAM) is one of the metal additive manufacturing method in which rapid fabrication of complex parts and large size components is possible. The main challenges in WAAM process are residual stress formation, distortions, surface finish and non-uniform mechanical properties from top to bottom layers. Experimental research has been done from past decades to reduce residual stress and defects like crack formation. For this experimental analysis, in predicting optimized process parameters, usage of material, manufacturing time and economic conditions are undesired factors. So, a finite element model is modelled to predict any mechanical and thermal property for the parts produced using WAAM process.

2.2 The objectives of this research work are:

- Theoretical Analysis of temperature distribution and phase transition of Ni-Ti alloy with respect to the temperature.
- Finite Element Modelling of Goldak Heat Source model to simulate WAAM process.
- Develop a computational WAAM model in which parameters gets changed with inter-pass time and temperature.
- Develop a WAAM model which can predict output thermal and mechanical parameters like temperature distribution, residual stress Von-Mises stress, etc.,
- To perform experimental analysis to validate the developed WAAM model.

- To observe the differences between the theoretical study and experimental study to analyze the possible causes for the variation.

2.3 Research Methodology

The research methodology used for our process work

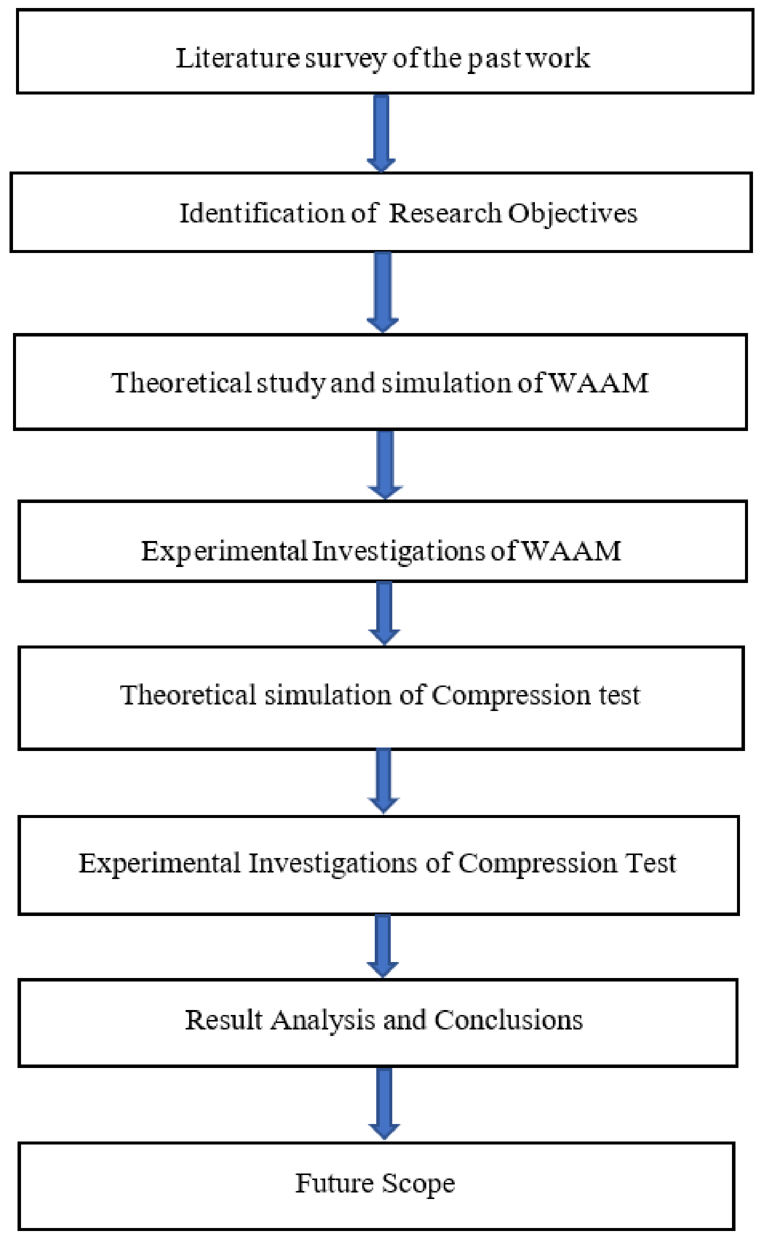

Fig 2.1 Research Methodology

2.4 Outline of thesis work

Chapter 3 describes about the literature survey of many research papers and books related to our research work. The numerical models to simulate WAAM which are developed in the past work, experimental analysis with material behaviour of Ni-Ti alloy, parameters and limitations to be considered to obtain efficient end components etc., have been reviewed through this literature study.

Chapter 4 describes about the detailed procedure of numerical modelling of WAAM process. The thermal study of phase transition of Ni-Ti alloy, input parameters, boundary conditions, formulas from literature survey, standard geometrical model design and the simulation of WAAM process are discussed here.

Chapter 5 describes about the experimental analysis of WAAM process with detailed explanation. The process parameters, machine setup, G code programming, various cooling times, preheating are discussed in this chapter.

Chapter 6 discusses about the uniaxial compression test of produced samples and also validating them with numerical simulation. In this chapter, discussion regarding cutting the samples to specific size and performing compression test is done.

Chapter 7 gives the detailed explanation about the results obtained from all the theoretical and experimental investigations. The causes of the variation in results are discussed here with reasonable conclusions and briefing about the future scope of this research work.

CHAPTER - 3

LITERATURE REVIEW

J. Goldak et al [1] proposed a new finite element model to develop a moving heat source model for the simulation of welding and other similar processes. A power density function is developed mathematically which is of Gauss distribution to develop a novel approach of moving heat source model. In many arc-welding processes and laser process, an in-depth penetration or deep heat distribution of the substrate or joint will take place, so to numerically define these type of heat distributions a double ellipsoid heat source model is developed. This GOLDAK double heat source model gives accurate results when compared with other literature works and this heat source model is used widely for simulation of many manufacturing processes.

F. Montevecchi et al [2] has performed finite element analysis in simulating the WAAM process which is similar to actual WAAM process. This thermo-mechanical analysis is done numerically by defining all the material parameters with respect to temperature. Also, a new moving heat source is modelled to replicate the actual power distribution in between the substrate and feed stock wire. Element-Birth technique is implemented numerically corresponding to the movement of the heat source to simulate the deposition process. This computational model is then validated by performing the experiment and found that with exceptional inaccuracies, the finite element model provides accurate results similar to experimental results. This model can be used to predict residual stress, distortions and also required heat source parameters by not performing any time-consuming experiments.

R. Tangestani et al [4] has developed a computational WAAM model to validate their numerical study with experimental results such that the developed WAAM model can be used to predict the residual stresses due to rolling without performing the experiment. The WAAM model developed is of stainless steel (SS) material upon structural steel substrate, the layers are deposited with the movement of heat source over the defined path. From this computational model, thermo-mechanical properties can be achieved and used for analysis to predict the residual stress of end component. These numerical results are then validated by performing the experiment with same material and parameters. The validation results are approximately similar and this research model can be used without going for experiment thing.

F. Montevecchi et al [3] proposed a finite element model with novel strategy to avoid or reduce the major collapse of the WAAM structures. An algorithm is developed with defined idle times in between each layer of deposition so that the inter-pass temperature and cooling of the workpiece is maintained. This finite element model is based upon the heat transfer equations and thermal study of the developed WAAM model. The experimental data is then compared with the numerical simulation to verify the accuracy of the finite element model. The proposed finite element technique showed efficient results in maintaining constant size of the weld pool and also the inter-pass temperature.

Z. Zeng et al [10] have done research on deposition of Ni rich Ni-Ti wire upon Ni-Ti substrate through WAAM process using Tungsten inert gas welding heat source (TIG) to study the changes in micro-structure, super elasticity, composition difference of the deposited layers from bottom to top. At the top layer, equiaxed grains were observed but at bottom layers columnar grains were observed and also the composition of Ni over the deposited layers is different. In the X ray diffraction analysis, it was observed that the built walls are present in austenite phase at room temperature, exhibiting superelasticity.

N. Resnina et al [5] have done research on deposition of Ni-Ti alloy over Ti substrate through WAAM process to study the changes in micro-structure, composition difference and variation of transformation temperature of martensite over the deposited layers from bottom to top. At the top layer, equiaxed grains were observed but at bottom layers columnar grains were observed and also the composition of Ni over the deposited layers is different. The bottom layers are mostly rich in Ti composition and due to this various composition of Ni-Ti, different martensite transformation temperature, the shape memory effect shows different deformation when compared to pre-deformed Ni-Ti sample.

J. Venkatesan et al [9] has developed a finite element model to predict the dynamic effects of boron carbide ceramic material like distribution of stress, material behaviour, strain at which the failure takes place by using elastic properties. The experimental and modelled test specimens are of cylindrical and cubical shape and the test setup used is modified split Hopkinson pressure bar (MSHPB). Gradual increase of material strength is observed with increase in strain rate under uniaxial compression test.

A. Saigal et al [8] has done a research study on Ni-Ti SMA compressive forces under strain-controlled environment. It was found that the compressive forces of superelastic SMA Ni-Ti wire (Ni – 55%, Ti – 45%) is more than tensile forces. This research describes about the shape recovery characteristic behaviour of Ni-Ti (bulk material) under compressive deformation. The strain ratio obtained is 1:57, and the average values of the strain of martensitic transformation are 5.25% - 5.75% in tension, 3.25% – 3.75% in compression.

Dalibor V [7] studied the effect of heat treatment upon mechanical properties of shape memory alloy Ni-Ti. In this research, the nitinol wire was annealed at specified high temperature in between $410^{o}\mathrm{C}$ - $540^{o}\mathrm{C}$ with a time period of 2 – 16 minutes. Annealing was done in the furnace and then removed out to quench in the water at 20^{o}C. By using X-ray diffraction technique, the micro structure and grain size of the heat-treated Ni-Ti is observed, temperatures below 485^{o}C increased the strength upto some extent but above 485^{o}C the strength of the Ni-Ti wire gets reduced.

S. Shiva et al. proposed that annealing can be used to produce Ni-Ti shape memory alloys for Micro-Electro-Mechanical Systems (MEMS) through laser additive manufacturing with required homogeneous microstructure for predictive design and manufacturing of micro-electro-mechanical systems. numerical simulation and experimental research using a pulsed green laser were used to investigate laser annealing of laser additive-manufactured Ni-Ti constructions.

Dimitris C. Lagoudas [11] this research describes about the unique characteristics of SMA, which are different from other materials. Due to the extraordinary thermal and mechanical properties, SMA is a proprietary alloy that can change its shape and restore its original shape by increasing the temperature even after the load and stress is applied. SMA can be used as shock absorbers as it has the ability to absorb vibrations and shocks.

CHAPTER - 4

Theoretical Investigations on Laser Hybrid Wire Arc based Additive Manufacturing

4.1 Phase Transition Modelling

The study of phase transition of Ni-Ti alloy with respect to temperature during solidification is essential before going for finite element modelling. In WAAM process, the feed wire gets melted, deposited and solidifies over the substrate. This process of solidification in WAAM can be referred to casting process in which molten metal solidifies in a mould.

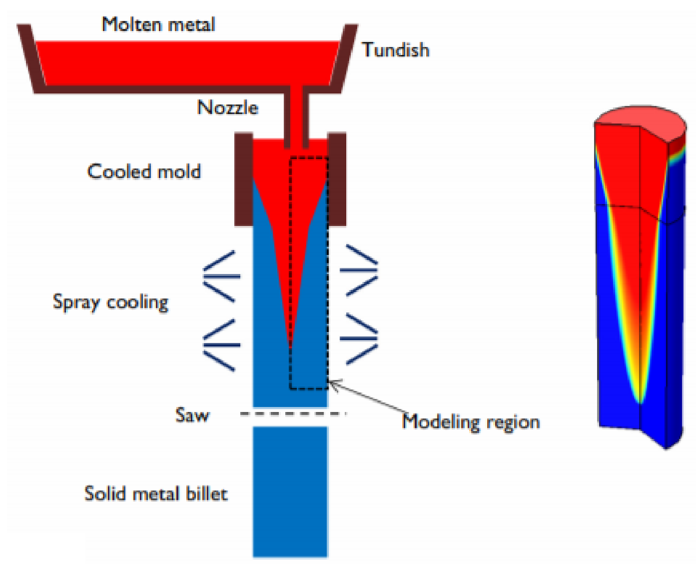

Fig 4.1 Phase Transition Modelling

To observe the phase transition of Ni-Ti alloy, thermal analysis is done in COMSOL 5.5 software. A two-dimensional (2 D) model of Ni-Ti alloy section is modelled with all the Ni-Ti properties defined in the parameters section. The input parameters can be referred from Table.

Table – 1: Input Parameters (Phase Transition)

Sr. No.	***Parameters***	***Input Value***
1	Melting Point Temperature (T_m)	$1275^{o}\ C$
2	Ambient Temperature (T_0)	$27^{o}\ C$
3	Heat Capacity, solid (C_p_s)	320 (J / kg-K)
4	Heat Capacity, liquid (C_p_l)	837 (J / kg-K)
5	Heat Transfer coefficient (h)	250 (W / m^2-K)
6	Latent heat of Solidification (dH)	224 (kJ / kg)
7	Surface Emissivity (∈)	0.66
8	Melt inlet temperature (T_in)	$1497^{o}\ C$

Fine mesh and coarser mesh are defined to observe the gradual transition between solid and liquid. Each solution after one iteration is considered as the starting point for the next iteration by using sharp transition.

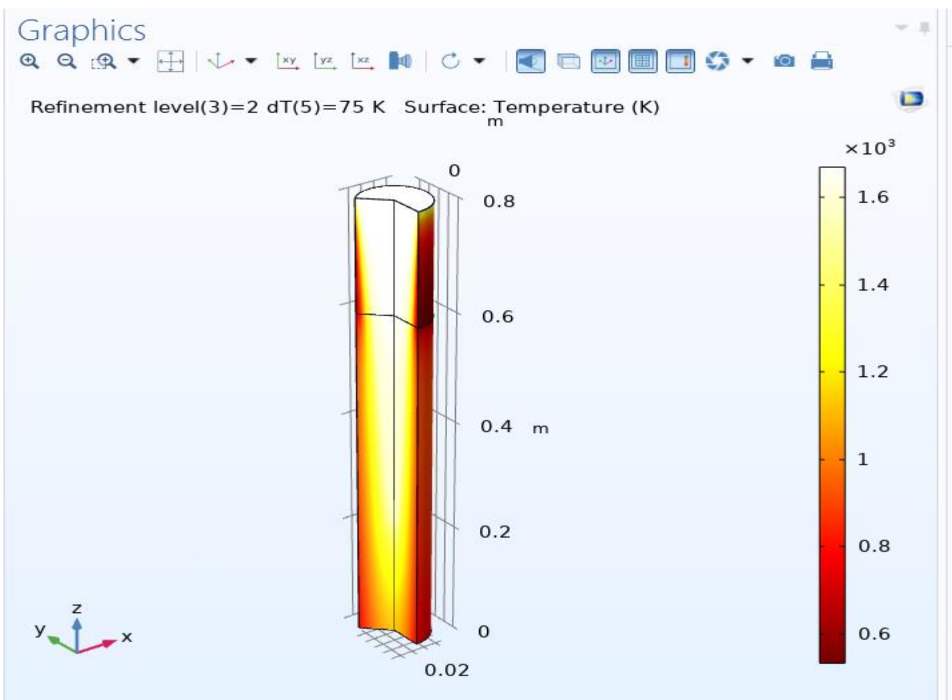

Fig 4.2 3-D Rotational view of the Ni-Ti wire

Adaptive mesh refinement algorithm is used to refine the mesh by generating more elements at the transition region and finds sharper transition zone for defined list of values (ΔT = 300 K, 200 K, 150 K, 100 K, 75 K). The results of the phase transition analysis were described in the results and discussion chapter.

4.2 WAAM Simulation

The simulation of the WAAM process can be used as a powerful tool to predict and tackle the defects obtained in the material deposition process. A finite element study is carried out to simulate the entire deposition process by modelling a moving heat source and addition of layers with respect to the movement of the heat source. Two kinds of finite element analysis are done to predict the final parameters of the WAAM process. Initially, thermal analysis is performed to obtain thermal parameters like heat flux distribution, temperature distribution which are used as input parameters for the mechanical analysis. After the mechanical analysis, parameters like mises stress, principal stress and residual stress of the component are obtained. Initially, numerical modelling is done by defining respective formulas from literature survey and then geometric modelling is done with respect to the dimensions. After modelling part is done, bed and wall material properties with respect to the temperature are defined for WAAM process simulation. DFLUX subroutine is used to simulate the moving heat source and also PYTHON SCRIPT is introduced for the layer-by-layer deposition of material.

4.3 Numerical Modelling and work-flow chart

ABAQUS 6.20 SOFTWARE is used to carry out the numerical simulation of WAAM process. The base plate of titanium material is modelled with dimensions of 100 X 60 $\mathbf{mm^2}$.

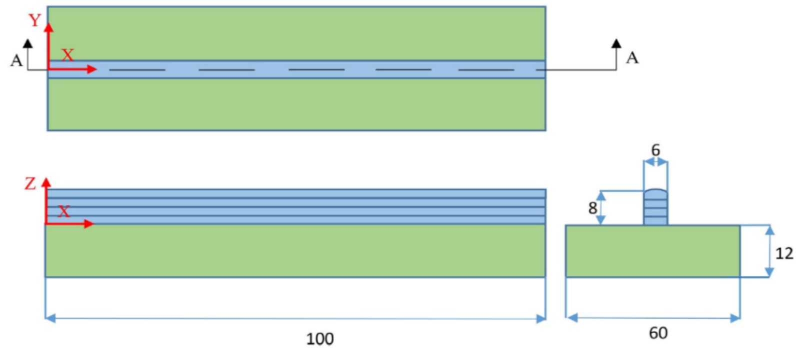

Fig 4.3 Dimensions of the WAAM model

When the thermo-mechanical finite element analysis is carried out, it is defined to avoid the nodes of the base plate from moving towards the transverse direction.

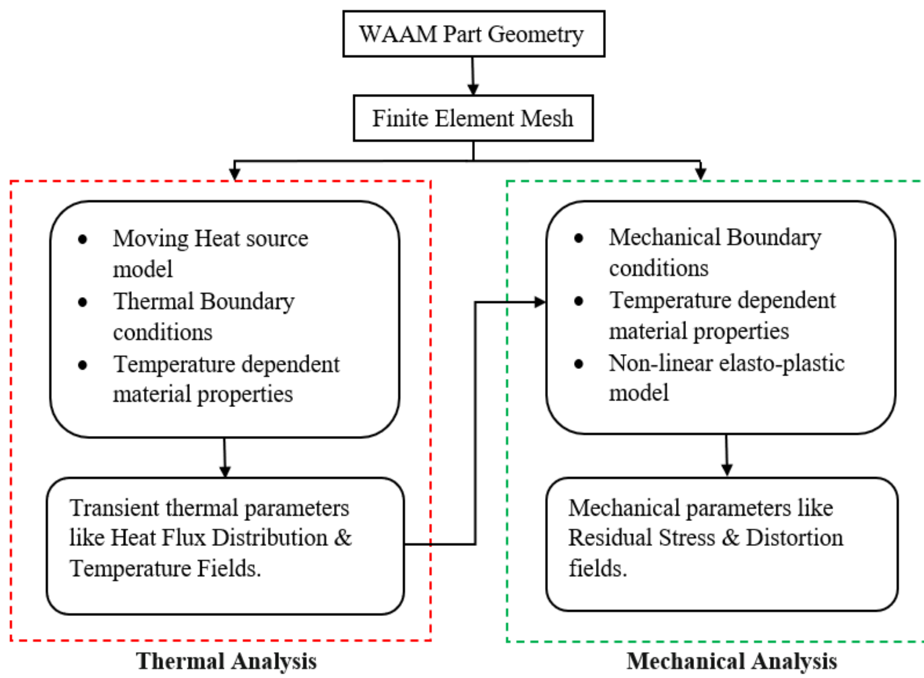

Fig 4.4 Thermo-Mechanical analysis flowchart

The GOLDAK heat input model is developed numerically for this simulation. To model this GOLDAK heat source, the DFLUX subroutine is used to define the ellipsoidal parameters, and heat source equations with respect to time. The elements of the wall were deactivated in the initial step and when the heat source model moves over the base plate, the elements get activated sequentially.

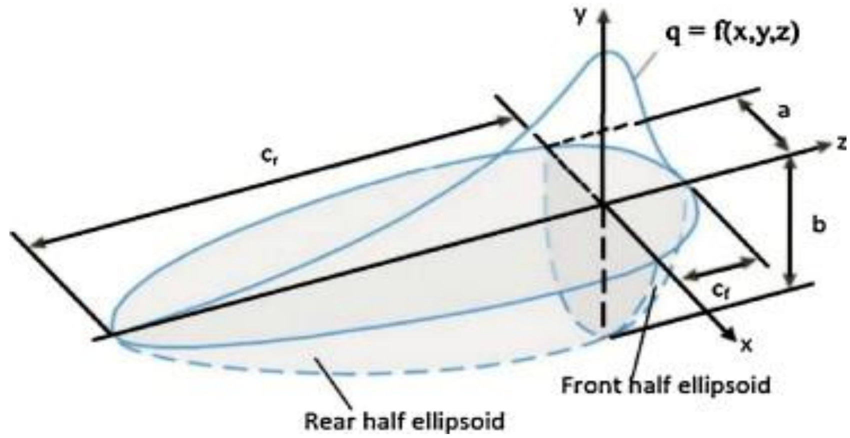

Fig 4.5 Goldak double ellipsoid model

Goldak heat source equations

- q_f (x, y, z, t) = $\frac{6*\sqrt{3}*Q*f\_f}{a*b*c*\pi*\sqrt{\pi}}*e^{[-3*\left(\frac{x}{a}\right)^2+\left(\frac{y}{b}\right)^2+\left(\frac{\varepsilon}{c\_f}\right)^2]}$
- q_r (x, y, z, t) = $\frac{6*\sqrt{3}*Q*f\_r}{a*b*c*\pi*\sqrt{\pi}}*e^{[-3*\left(\frac{x}{a}\right)^2+\left(\frac{y}{b}\right)^2+\left(\frac{\varepsilon}{c\_r}\right)^2]}$
- a = 3 mm, b = 2.5 mm, c_f = 2 mm, c_r = 6 mm

Where ε = z + ν*($\tau - t$) and a, b, c_f, c_r are ellipsoidal parameters.

q_f – Front ellipsoid heat flux

q_r – Rear ellipsoid heat flux

Boundary conditions of heat source modelled,

$$q\ (x, y, z, t) = \begin{cases} q\_f\ for\ z \geq z0 \\ q\_r\ for\ z < z0 \end{cases} \quad \text{and}$$

$$\frac{f\_f}{c\_f} = \frac{f\_r}{c\_r}$$

where f_f + f_r = 2.

Heat input - Q = η*I*V (in Watts)

Table – 2: Input Process Parameters (WAAM)

Sr. No.	***Parameters***	***Input Value***
1	Heat Input (Q)	1031.25 W
2	Input Current (I)	125 A
3	Input Voltage (V)	16.5
4	Heat transfer efficiency (η)	50 %
5	Heat fraction Coefficient (front, f_f)	0.6 mm
6	Heat fraction Coefficient (rear, f_r)	1.4 mm
7	Velocity (v)	8.33 (mm / s)

Very fine mesh and small element size is used to obtain accurate results of the simulation. The "element birth technique" was used to show the deposition of layers.

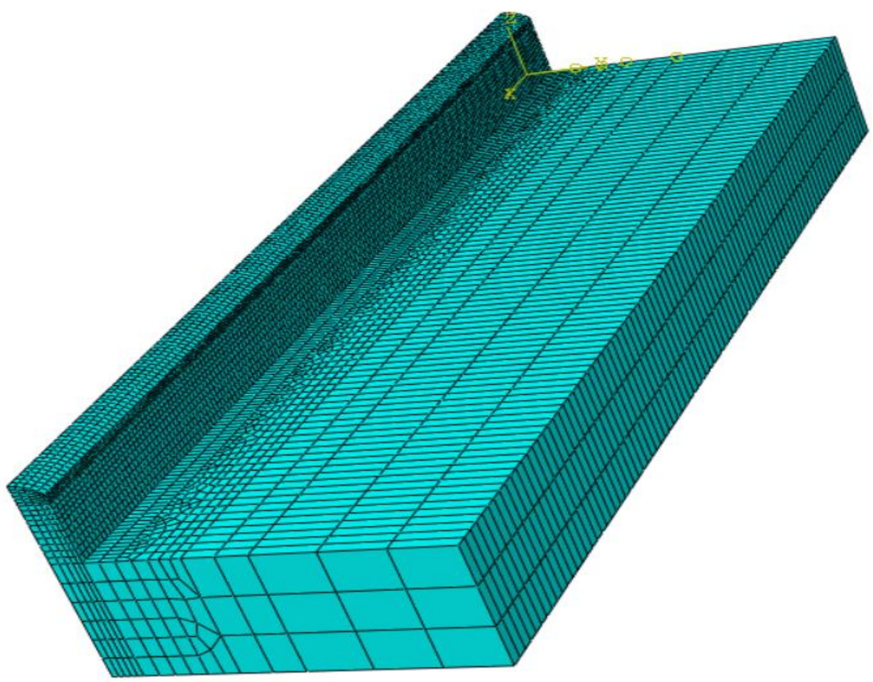

Fig 4.6 Meshed WAAM model

PYTHON script is used to define the steps and time increments that are required for the deposition of layers corresponding to time. This PYTHON script and DFLUX subroutine are then integrated with ABAQUS 6.20 software to run the job analysis. The wire feed speed and heat source travel speed were 10 m/min and 8.33 mm/s. The heat input is of 1631.25 W, with the cooling time of 10 s, 20 s and 30 s which is defined in between each layer of deposition**.**

The thermal parameters like temperature distribution, heat flux distribution etc., and mechanical parameters like von mises stress, principal stress, residual stress etc., can be obtained at each and every step of increment throughout the entire simulation of WAAM process. The results of the thermo-mechanical analysis obtained are described in chapter-5.

4.4 Preheating

To reduce the residual stress and distortions, cooling time is provided in between the layer deposition within the WAAM process but there exists another method which can reduce the residual stress of the end component. "Preheating" can be done to the base plate or bed before the deposition of the wall material over the base plate. The required temperature can be defined for the initial preheating and this technique promises in showing desired results i.e., less distortions and residual stress.

The substrate i.e., Ti plate is initially preheated to $200^{o}\mathrm{C}$ and then the Ni-Ti wire is deposited on the base plate. In numerical simulation, it is to define the preheating thing i.e., just by defining the initial temperature of the base plate as $200^{o}\mathrm{C}$ instead of $25^{o}\mathrm{C}\ (\mathrm{i.e., room\ temperature})$. The procedure to simulate the preheating of WAAM is similar to the previously mentioned section i.e., numerical analysis of various cooling times. The results of the preheating analysis were described in the results and discussion chapter.

The titanium plate is initially preheated before the Ni-Ti deposition. Deposition begins after preheating temperature is achieved. Each layer was built in 12 s with a 10 s pause between deposition of the consecutive layers. The pause enabled the sample to cool down before new layers were deposited.

CHAPTER – 5

Experimental Investigations on Wire Arc based Additive Manufacturing

5.1 Experimental Procedure for various cooling times

The Ni-Ti wire of 0.8 mm diameter is used as feedstock material and the baseplate is of Titanium material. The wire arc additive manufacturing (WAAM) process follows the technique of Metal Inert Gas Welding (MIG) to deposit the SMA wire upon the titanium plate. The WAAM equipment consists of argon gas cylinder, wire feeder to feed the wire during deposition, computer for programming, work bench for positioning and a transformer to control voltage and current. The electric arc as fusion along with wire feeder is WAAM process.

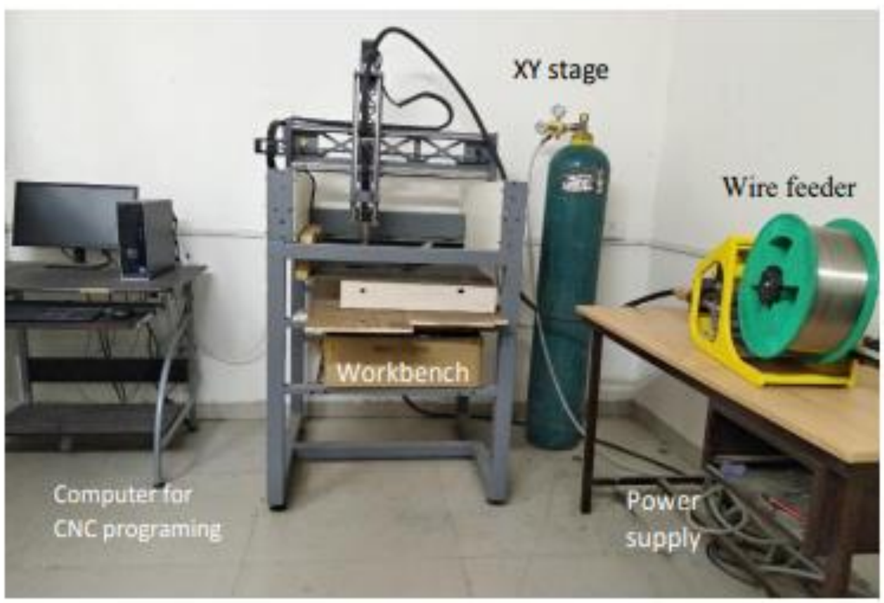

Fig 5.1 WAAM Setup

The argon gas cylinder is used for shielding purpose to avoid chemical oxidations. The computer is used for positioning of nozzle in X, Y & Z axis by programming through G codes within the Repitier host software.

Table – 3: Optimized parameters for the WAAM Deposition

Wire feed rate (m/min)	Argon gas flow rate (L/min)	Voltage (V)	Current (A)
10	15	16.5	125

Fig 5.2 Experimental Samples of 10 sec, 20 sec & 30 sec cooling time

While depositing the layers ensure that less defects are present in the end component. Defects like crack propagation, delamination of the deposited wall from the base plate, distorted shapes, spatter formation etc., will takes place. The WAAM machine is semi-automatic setup and the deposition takes place by operating through a manual switch at the nozzle. The nozzle positioning, movement in X, Y, Z axis and cooling time between deposition are controlled by the program in the computer. The operating of the switch has to be perfect and accurate with respect to the G-codes program to avoid overlapping and non-linearity of layers. The G-code program is developed for the deposition of about 10 layers over the base plate. The heat generated in this process is too high, which causes the Ni-Ti wire to get clogged inside the nozzle. The same experimental procedure is repeated for three samples of three different cooling times 10, 20 and 30 seconds.

5.2 Experimental Procedure for preheating

For the reduction of residual stresses and distortions, the preheating is done. The heating of the substrate can be done by the heater plate of the WAAM setup which can be adjusted manually to required temperature.

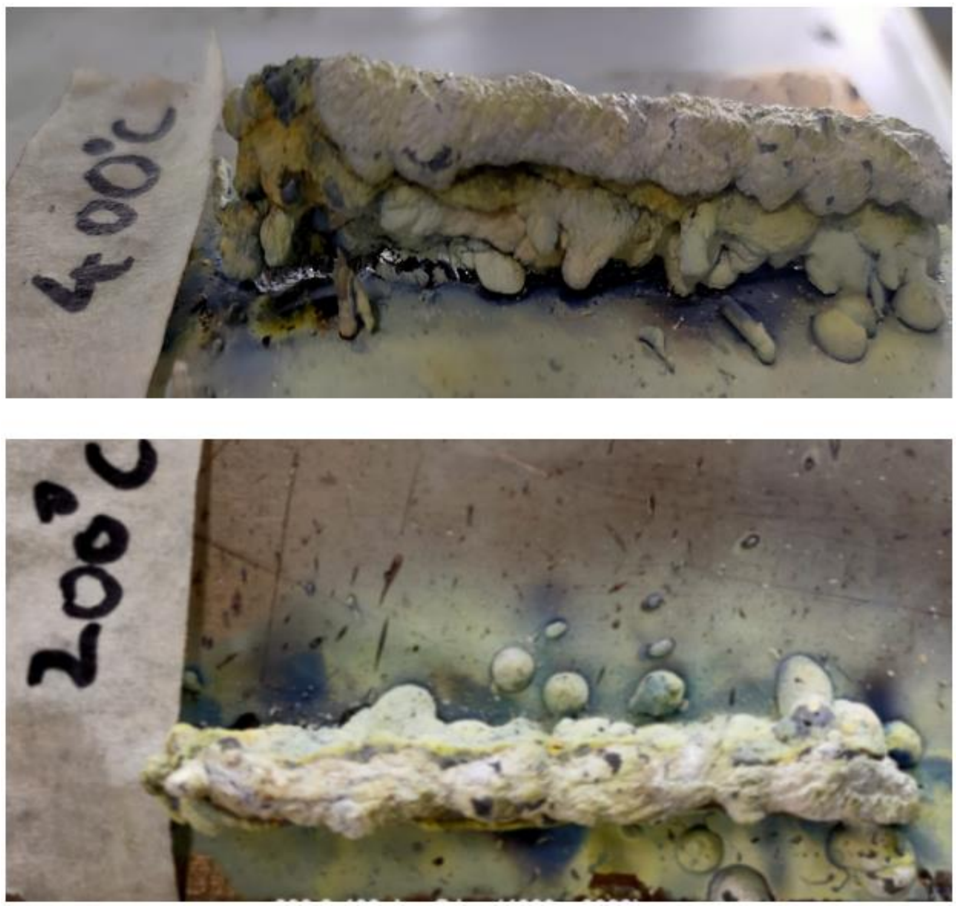

Fig 5.3 Preheating Samples of $200^{o}C$ and $400^{o}C$

For our research purpose, the preheating temperatures defined are 200^{o}C and 400^{o}C respectively. The process parameters to perform this WAAM experiment are described in table 1.

Table - 4: WAAM process parameters

Sr. No.	Initial Temperature	Delay (in sec)	Substrate	Wire	No. of layers
1	$25^{o}C$	10	Ti	Ni-Ti	10
2	$25^{o}C$	20	Ti	Ni-Ti	10
3	$25^{o}C$	30	Ti	Ni-Ti	10
4	$200^{o}C$	10	Ti	Ni-Ti	10
5	$400^{o}C$	10	Ti	Ni-Ti	10

The samples are then cut into specific size and compression test is done to find out the strength of all samples. The result analysis of all the samples is compared with numerical simulation results and described in results and discussion chapter.

CHAPTER – 6

UNIAXIAL COMPRESSION TEST

The deposited samples are then cut into small pieces of size 6*3*3 mm^3 (ASTM standards) by using Wired Electrical Discharge Machining (WEDM), the required size dimensions are entered into the system and the entire cutting is done into cuboid shape by the machine automatically as it is a CNC machine. The end samples are then subjected to compression test to find out the compressive strength of each sample.

Fig 6.1 Shape Memory Effect and Super-elasticity

To find out the compression strength of a normal Ni-Ti sample, numerical simulation of compression test is modelled using FEM software. From this numerical simulation results, the compressive strength is then compared with experimental samples compressive strength, by performing compression test to observe the differences and variation due to cooling and preheating.

6.1 Numerical Modelling of Compression Test

To simulate the uniaxial compression test, a solid cylinder of Ni-Ti material is modelled. The numerical simulation is modelled similar to a concrete cylinder being compressed in Universal Test Machine (UTM).

Fig 6.2 Concrete cylinder under compression

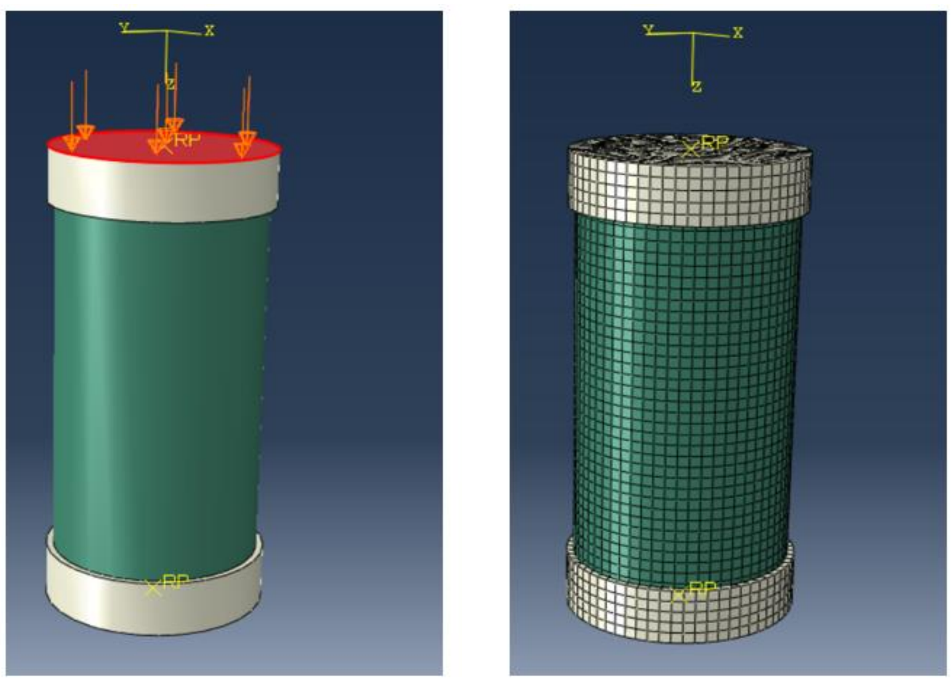

Fig 6.3 Ni-Ti cylinder

Very fine mesh is defined to obtain precise and accurate results. The mechanical properties of Ni-Ti which were used in WAAM simulation are defined within the ABAQUS software.

Table – 5: Input parameters (compression test)

Load (kN)	Cylinder	Density (kg/m^3)	Poisson's Ratio
10	Ni-Ti	6450	0.33

The required boundary conditions similar to uniaxial compression test are defined i.e., bottom plate fixed and load is applied from top cross-head.

6.2 Experimental Investigations on Compressive strength

The five samples which has been cut by WEDM process are now tested to measure their compressive strength. Compressive strength can be measured by Universal Testing Machine (UTM). The applied load is of 10 kN is applied and the stress developed can be seen digitally. The machine stops applying the load when the sample reaches fracture strength and the end value shown is the compressive strength of the sample.

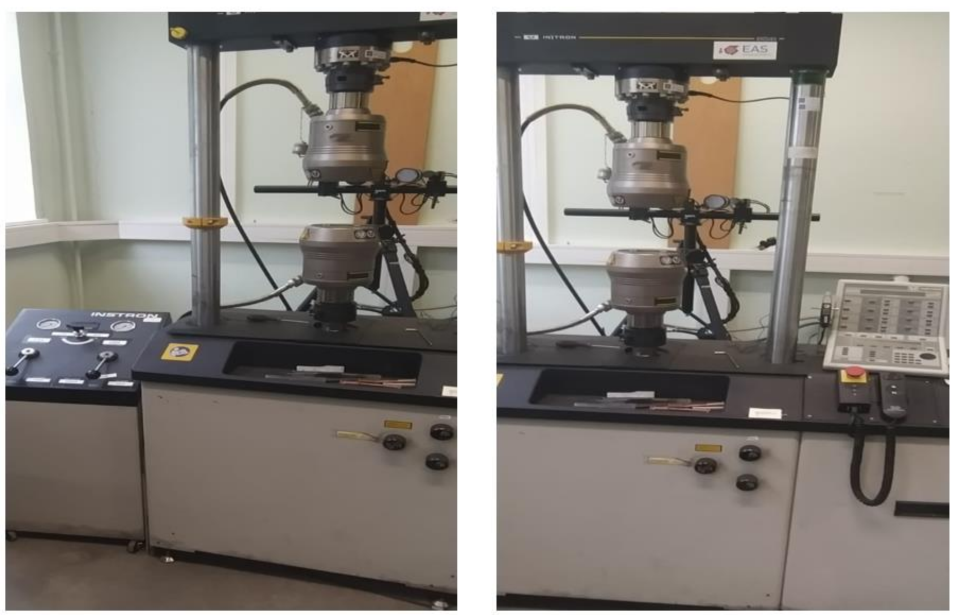

Fig 6.4 Universal Test Machine

CHAPTER - 7

RESULTS & DISCUSSION

7.1 Phase Transition Modelling of Ni-Ti results

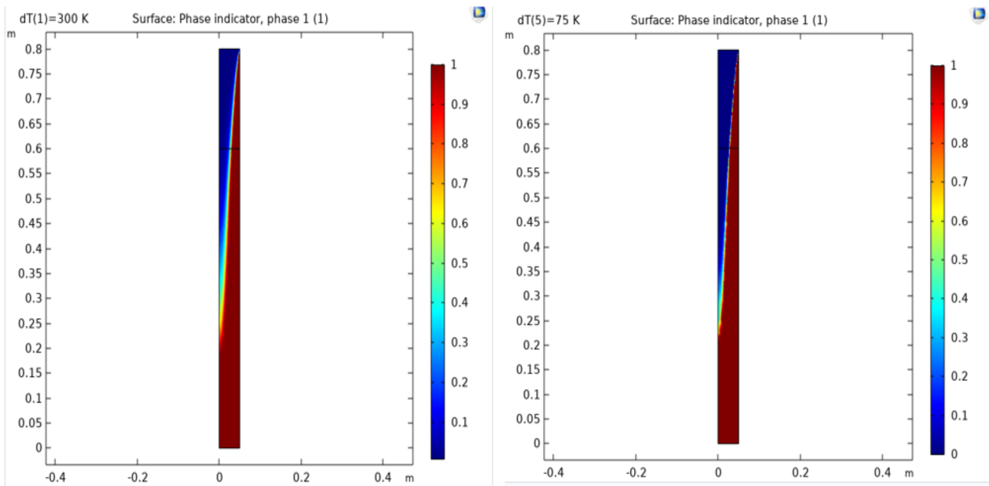

Fig 7.1 Ni-Ti Phase Transition

The solidification front of $\triangle T$ = 300K and $\triangle T$ = 75 K are shown in the above figures, which moves slightly as transition zone shrinks and a finer mesh is needed to converge the model. Phase indicator graphs for all the transition zones are plotted in 'r' and 'z' coordinates with respect to temperature.

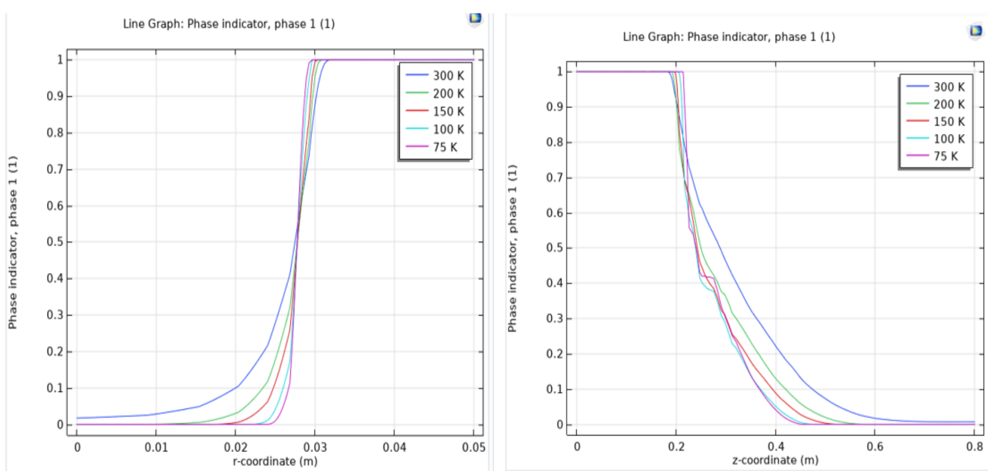

Fig 7.2 Graphs in 'r' and 'z' coordinates

7.2 Various cooling time results (10 sec, 20 sec, 30 sec)

To observe the temperature distribution within the WAAM component throughout the process, graphs are plotted for 10 s, 20 s & 30 s inter-pass cooling time.

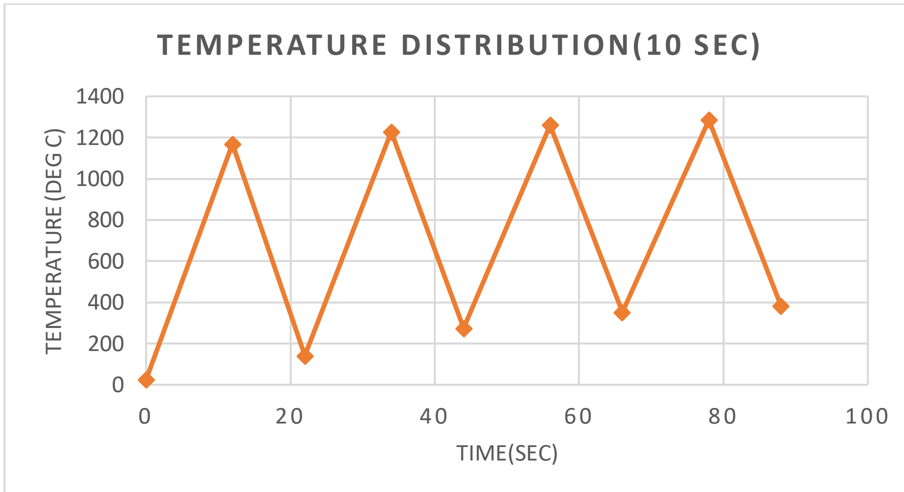

7.3 (a)

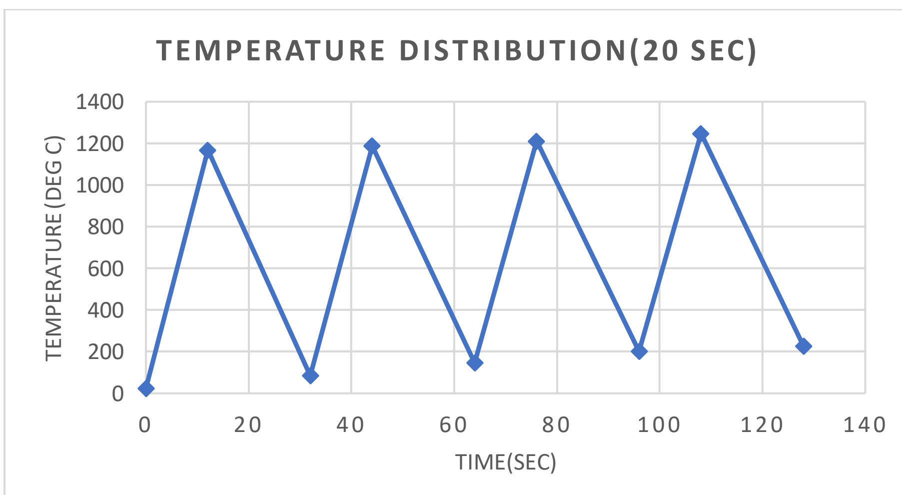

7.3 (b)

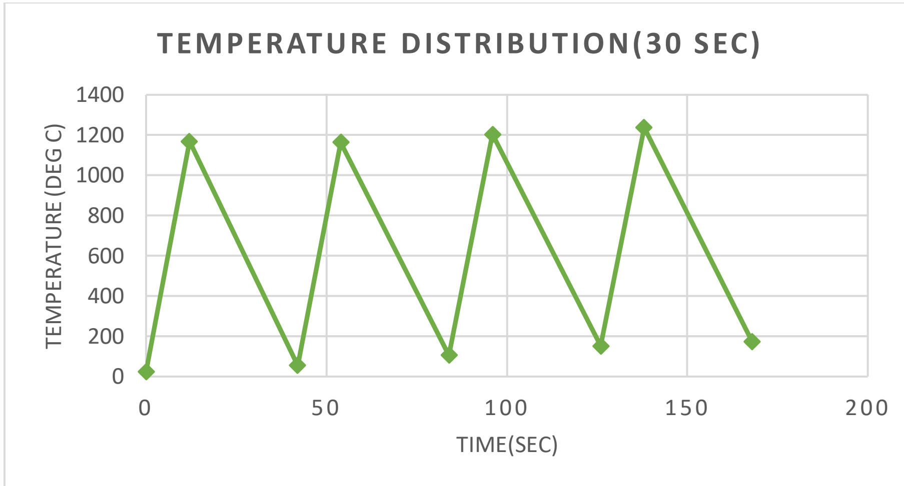

7.3 (c)

Fig 7.3 – (a), (b) and (c) are the temperature distributions of 10 sec, 20 sec and 30 sec cooling time of WAAM model

The lines climbing up and down with respect to the time indicates that the component temperature is raised while layer is getting deposited and after a layer is deposited during the inter-pass cooling time the component temperature is reduced. The temperature variation continues till the last layer is deposited.

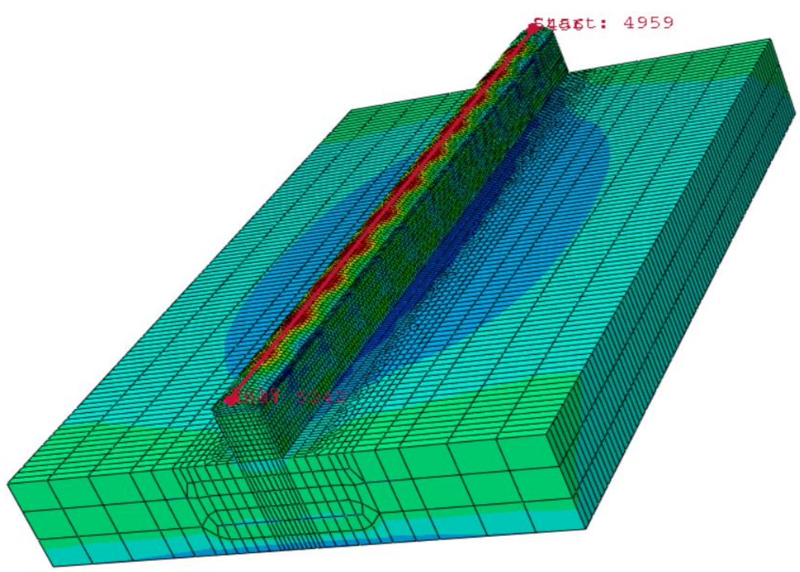

Fig 7.4 Centre-Line Path

The Residual stresses are caused by differential thermal expansion and contraction of the weld metal(wire) and parent material. If stress buildup in the weldment is excessive, the fatigue life of the component is reduced. Variation in the cooling rate from the mold wall to its center can cause thermal-induced residual stress.

The residual stress values along the centreline path for 10 s, 20 s & 30 s are plotted in single graph to observe the variation.

Among the three curves, the 30 s curve has less magnitude and 10 s curve has the highest magnitude when compared to others along the path.

Similarly, we can plot the graphs to observe desired mechanical and thermal properties like heat flux distribution, von mises stress, principal stress etc., variation along the path or with respect to the time.

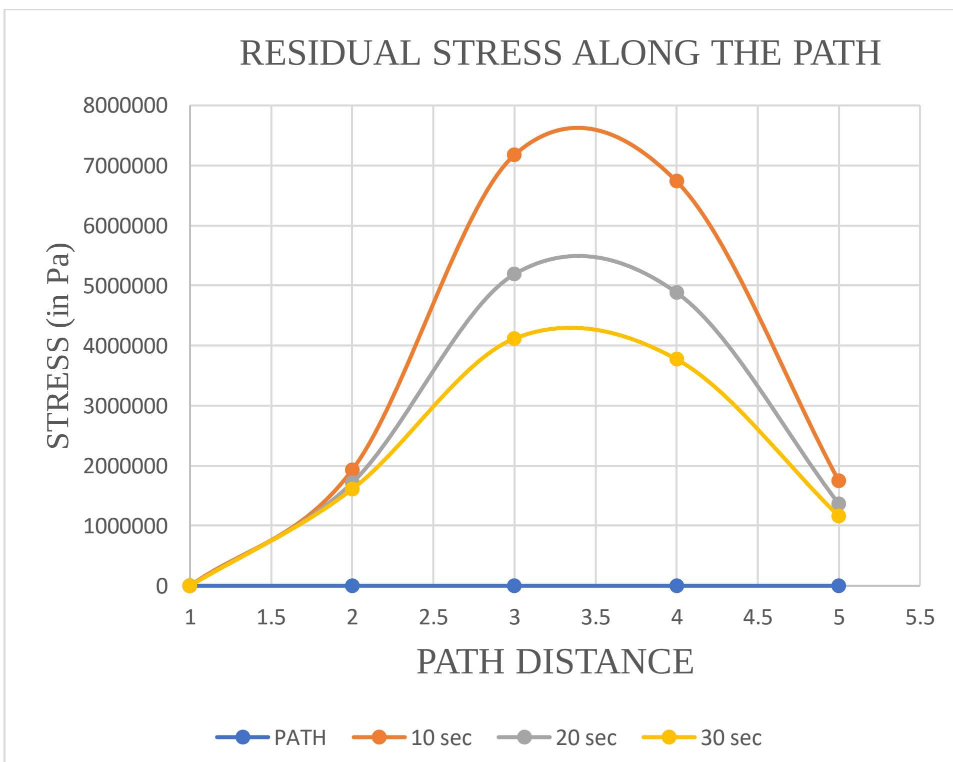

Fig 7.5 Residual Stress Variation

7.3 Preheating Results (200^oC and 400^oC)

The numerical modelling procedure followed for the preheating model is same as the FEM modelling of WAAM process which is described in the earlier sections. The preheated temperatures defined are 200^oC and 400^oC respectively to the WAAM model. The cooling time between each layer of deposition is 10 seconds for both the preheated models.

The residual stress values along the centreline path for WAAM model of 200^oC, 400^oC and non-preheated model (i.e., at room temperature 25^oC) are plotted in single graph to observe the variation.

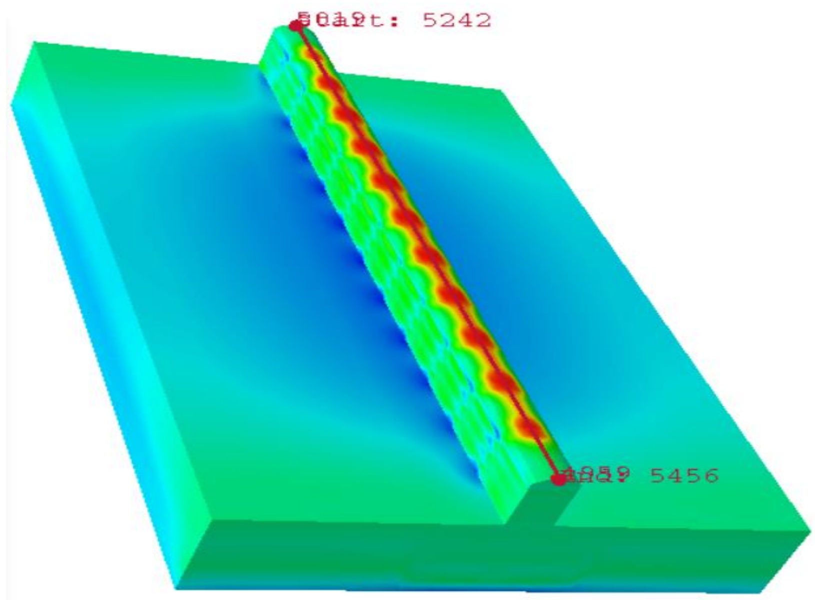

Fig 7.6 Centre-Line Path (Pre-heating)

Among the three curves, the preheating temperature of 400^oC curve has less magnitude and room temperature curve has highest magnitude when compared to others along the path.

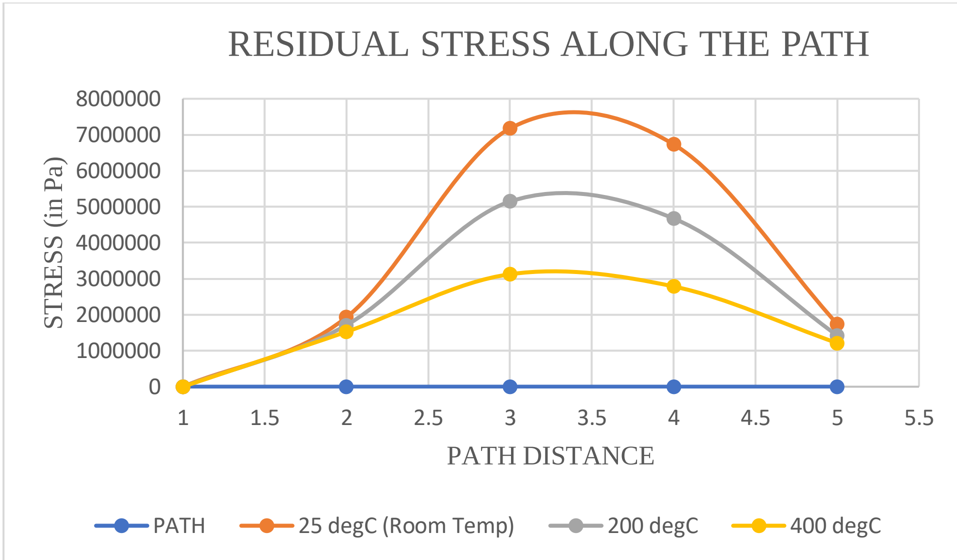

Fig 7.7 Residual Stress (Pre-heating)

7.4 Compression Test results

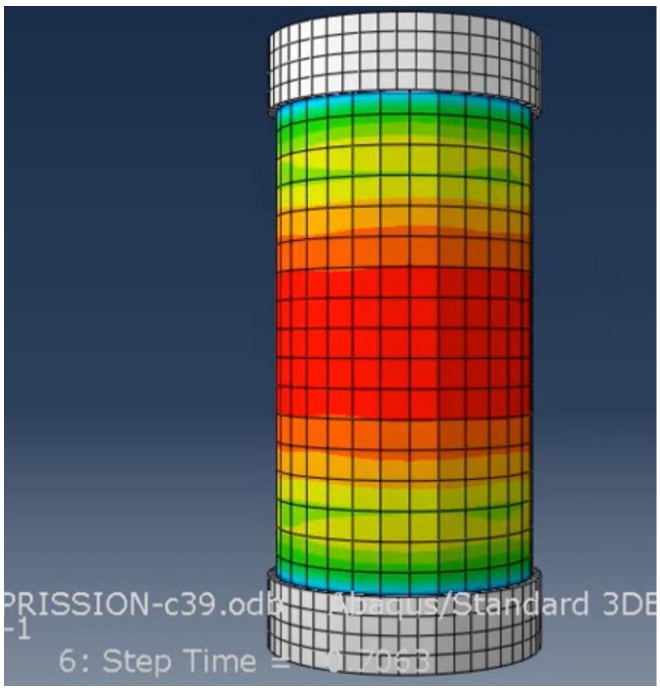

Fig 7.8 Compression Test Simulation

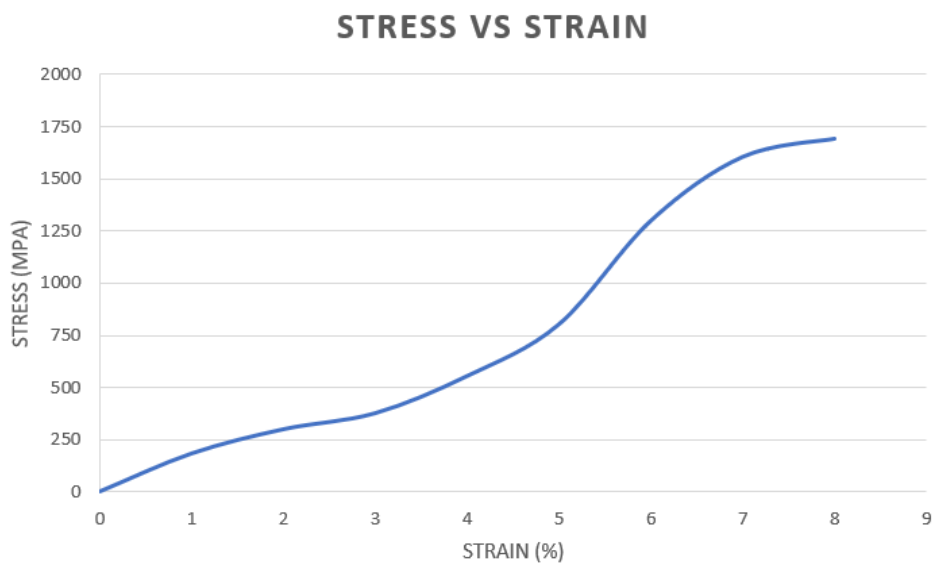

Fig 7.9 Stress-Strain Graph of Compression Test Simulation

7.5 Experimental Compression Test results

The compressive strength got reduced for higher cooling rates but with less cooling rates, deposition of desired number of stack of layers is becoming difficult. Crack formation and delamination from the base plate are the main issues with lower cooling times. With increase in cooling time, the deposited layer gets enough time to solidify and also the next layer can be deposited smoothly without any cracks or deformation.

Table – 6: Compressive Strength results

Sr. No.	Sample	Compressive Strength (MPa)
1	10 sec	2083
2	20 sec	1756
3	30 sec	1527
4	200°C	821
5	400°C	693

A sample size of standards like ASTM, ASME, BS etc., has been cut from the end part to measure the residual stress. By using Non-Destructive

Techniques (NDT) like X-Ray Diffraction (XRD) technique, Ultrasonic, Electro-Magnetic methods etc., residual stress of the end component can be measured.

CHAPTER – 8

CONCLUSIONS

8.1 Theoretical & Experimental Investigations on WAAM

These Residual stresses are caused by differential thermal expansion and contraction of the weld metal(wire) and parent material. If stress buildup in the weldment is excessive, the fatigue life of the component is reduced. Variation in the cooling rate from the mold wall to its center can cause thermal-induced residual stress.

The graphs of various cooling times and preheated temperature models are compared to observe the residual stress variation for both the cases. It is observed that the residual stress with preheating temperature of $400^{o}\mathrm{C}$ shows very low residual stress levels among all the cases and the non-preheated model of less cooling time induces high residual stress within the WAAM component.

In the experimental study, delamination and embrittlement of deposited wall from the base plate is one of the main issues faced in this preheating thing. If optimum preheating temperature with respect to the type of material is maintained, desired wall structures can be constructed without any issues.

8.2 Uniaxial Compression Test

In 30 sec cooling time, the wall structures are deposited without any defects of desired number of layers which became difficult for 10 sec and 20 sec. In contrast, the compressive strength got reduced and is of less magnitude for 30 sec cooling time. In the case of preheating, the compressive strength is reduced drastically when compared with non-preheated sample. Also, the delamination problem is faced many times in the case of preheating samples.

CHAPTER - 9

REFERENCES

1. John Goldak, Aditya Chakravarti, Malcolm Bibby, A new finite element model for welding heat sources, Metallurgical transactions B, 1984, 15, 299 - 305.
2. Filippo Montevecchi, Giuseppe Venturini, Antonio Scippa, Gianni Campatelli, Finite element modelling of Wire-Arc-Additive-Manufacturing process, Procedia CIRP, Volume 55, 2016, 109 - 114, doi: 10.1016/j.procir.2016.08.024.
3. Filippo Montevecchi, Giuseppe Venturini, Niccolo Grossi, Antonio Scippa, Gianni Campatelli, Idle time selection for wire-arc additive manufacturing: A finite element-based technique, Additive Manufacturing, Volume21, 2018, 479 - 486, doi: 10.1016/j.addma.2018.01.007.
4. Reza Tangestani, G H Farrahi, M Shishegar, B P Aghchehkandi, S Ganguly, Ali Mehmanparast, Effects of Vertical and Pinch Rolling on Residual Stress Distributions in Wire and Arc Additively Manufactured Components, Journals of Material Engineering and Performance, 2020, 29, 2073 – 2084.
5. N. Resnina, I.A. Palani, S. Belyaev, S.S. Mani Prabu, P. Liulchak, U. Karaseva, M. Manikandan, S. Jayachandran, V. Bryukhanova, Anshu Sahu, R. Bikbaev, Structure, martensitic transformations and mechanical behaviour of Ni-Ti shape memory alloy produced by wire arc additive manufacturing, Journal of Alloys and Compounds, Volume 851, 2021, 156851, doi: 10.1016/j.jallcom.2020.156851.
6. Christian Scheitler, Oliver Hentschel, Thomas Krebs, Konstantin Yu. Nagulin, Michael Schmidt, Laser metal deposition of Ni-Ti shape memory alloy on Ti sheet metal: Influence of preheating on

dissimilar build-up, Journal of Laser Applications 29, 022309 (2017); doi: 10.2351/1.4983246

7. Dalibor Vojtech, Influence of Heat Treatment of Shape Memory Ni-Ti alloy on its mechanical properties, Materials Engineering 18, 2010.
8. Anil Saigal, Matthew Fonte, Solid, shape recovered “bulk” Nitinol: Part I—Tension–compression asymmetry, Materials Science and Engineering A, 528, 2011, 5536 – 5550, doi: 10.1016/j.msea.2011.03.060.
9. J. Venkatesan, M.A. Iqbal, V. Madhu, Experimental and numerical study of the dynamic response of B4C ceramic under uniaxial compression, Thin-Walled Structures, 154, 2020, 106785, doi: 10.1016/j.tws.2020.106785.
10. Z. Zeng, B. Q Cong, J. P. Oliveira, W. C Kea, N. Schell, B. Peng, Z. W. Qi, F. G Ge, W. Zhang, S. S. Ao, Wire and arc additive manufacturing of a Ni-rich Ni-Ti shape memory alloy: Microstructure and mechanical properties, Additive Manufacturing, 32, 2020, 101051, doi:10.1016/j.addma.2020.101051.
11. Dimitris C. Lagoudas**,** Thermo-Mechanical Characterization of Shape Memory Alloy materials, in: 2008: pp. 53–119.
12. B.I.T. Sindri, RESEARCH ARTICLE FUTURE OF SHAPE MEMORY ALLOY AND ITS UTILIZATION * Roy, Int. J. Curr. Res. Vol. 8 (2016) 31646–31651.
13. S. Jiang, J. Yu, L. Hu, Y. Zhang, Investigation on Deformation Mechanisms of Ni-Ti Shape Memory Alloy Tube under Radial Loading, Metals (Basel). 7 (2017) 268. doi:10.3390/met7070268.
14. H. Geng, J. Li, J. Xiong, X. Lin, Optimization of inter-pass temperature and heat input for wire and arc additive manufacturing

5A06 aluminium alloy, Sci. Technol. Weld. Join. 22 (2017) 472–483.doi:10.1080/13621718.2016.1259031.

15. Dimitris_C_Lagoudas, Shape Memory Alloys Modeling and Engineering Applications, 2007.
16. S. Hamidreza, J. Corker, M. Fan, Additive manufacturing technology and its implementation in construction as an eco-innovative solution Automation in Construction Additive manufacturing technology andits implementation in construction as an eco-innovative solution, Autom. Constr. 93 (2018) 1–11. doi: 10.1016/j.autcon.2018.05.005.
17. S. Kapil, F. Legesse, P. Kulkarni, P. Joshi, A. Desai, K.P. Karunakaran, Hybrid-layered manufacturing using tungsten inert gas cladding, Prog. Addit. Manuf. 1 (2016) 79–91. doi:10.1007/s40964-016-0005-8.
18. K.P. Karunakaran, S. Kapil, H. Vithasth, F. Legesse, Additive manufacturing of H13 tooling element with conformal cooling channel using MIG cladding, Int. J. Rapid Manuf. 7 (2018) 1. doi:10.1504/ijrapidm.2018.10010809.
19. M.-T. Le, Y.-U. Sohn, J.-W. Lim, G.-S. Choi, Effect of Sputtering Power on the Nucleation and Growth of Cu Films Deposited by Magnetron Sputtering, Mater. Trans. 51 (2009) 116–120. doi:10.2320/matertrans.m2009183.
20. J.H. Boo, M.J. Jung, H.K. Park, K.H. Nam, J.G. Han, High-rate deposition of copper thin films using newly designed high-power magnetron sputtering source, Surf. Coatings Technol. 188–189 (2004) 721–727. doi: 10.1016/j.surfcoat.2004.07.005.
21. S.W. Williams, F. Martina, A.C. Addison, J. Ding, G. Pardal, P. Colegrove, Wire + Arc Additive Manufacturing, Mater. Sci. Technol. 32 (2016) 641–647.

22. N. Knezovi, New Technologies, Development and Application, 42 (2019) 0–7. doi:10.1007/978-3-319-90893-9.
23. Y. Zhai, D.A. Lados, J.L. Lagoy, Additive Manufacturing: Making imagination the major Limitation, Jom. 66 (2014) 808–816. doi:10.1007/s11837-014-0886-2.
24. Näsström, J., Brueckner, F., & Kaplan, A. F. (2019). Laser enhancement of wire arc additive manufacturing. Journal of Laser Applications, 31(2), 022307.
25. Venturini, G., Montevecchi, F., Scippa, A., & Campatelli, G. (2016). Optimization of WAAM deposition patterns for T-crossing features. Procedia CIRP, 55, 95-100.
26. Xiong, J., Yin, Z., & Zhang, W. (2016). Closed-loop control of variable layer width for thin-walled parts in wire and arc additive manufacturing. Journal of Materials Processing Technology, 233, 100-106.
27. Pardal, G., Martina, F., & Williams, S. (2019). Laser stabilization of GMAW additive manufacturing of Ti-6Al-4V components. Journal of Materials Processing Technology, 272, 1-8.
28. Karbasi, H. (2010). COMSOL assisted simulation of laser engraving. In Proceedings of the Comsol Conference, Boston.
29. Piekarska, W., & Kubiak, M. (2012). Theoretical investigations into heat transfer in laser-welded steel sheets. Journal of thermal analysis and calorimetry, 110(1), 159-166.
30. Riahi, M., Hoseinpour Gollo, M., & Nader Ameli Kalkhoran, S. (2014). Experimental and numerical study of heat flux distribution in laser forming of bi-layer sheets. Journal of Computational & Applied Research in Mechanical Engineering (JCARME), 4(1), 67-79.

31. Nikolidakis, E., & Antoniadis, A. (2019). FEM modeling simulation of laser engraving. The International Journal of Advanced Manufacturing Technology, 105(7), 3489-3498.